Supporting Information for

A series of dynamic single crystals of $[M^{II}(en)_3]SO_4$ (M = Ni , Mn, Cd) shows tunable dielectric property and anisotropic thermal expansion

Cong Wu,[a] Kai-Ge Gao,[b] Zi-shuo Yao,*[a] and Jun Tao*[a]

[a]Key Laboratory of Cluster Science of Ministry of Education, School of Chemistry and Chemical Engineering, Liangxiang Campus, Beijing Institute of Technology, Beijing 102488, People's Republic of China.

[b]College of Physical Science and Technology, Yangzhou University, Yangzhou, Jiangsu 225009, People's Republic of China.

E-mail: zishuoyao@bit.edu.cn taojun@bit.edu.cn,

Table of Contents

IR Spectra.

Fourier transform infrared (FT-IR) spectra were recorded in the range of 4000 – 400 cm^{-1} on a Bruker ALPHA FT-IR spectrometer.

TG.

Thermogravimetric analyses (TGA) were carried out from 30 ℃ to 800 ℃ on a TG-DTA 6200 instrument under N_2 atmosphere with a heating rate of 10 K min^{-1}.

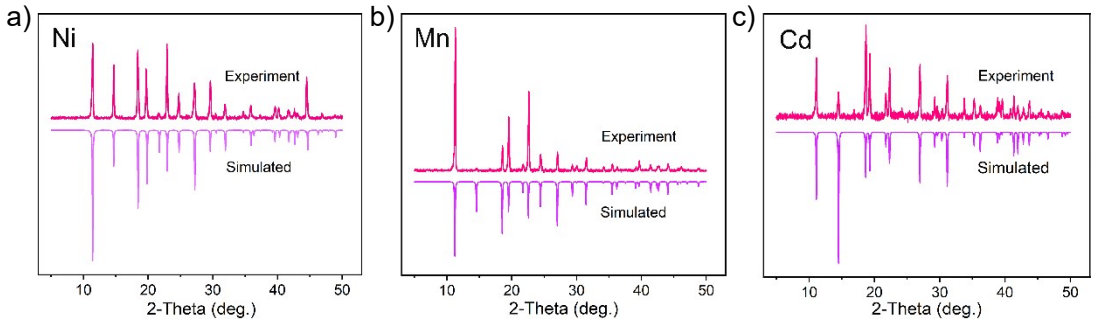

Figure S1. Comparison of the PXRD patterns of **1** (a), **2** (b), and **3** (c) powders (Experiment) with the single crystal structure fitting (Simulated) at room temperature. The experimental results are consistent with the simulation results, which proves the phase purity of the three complexes.

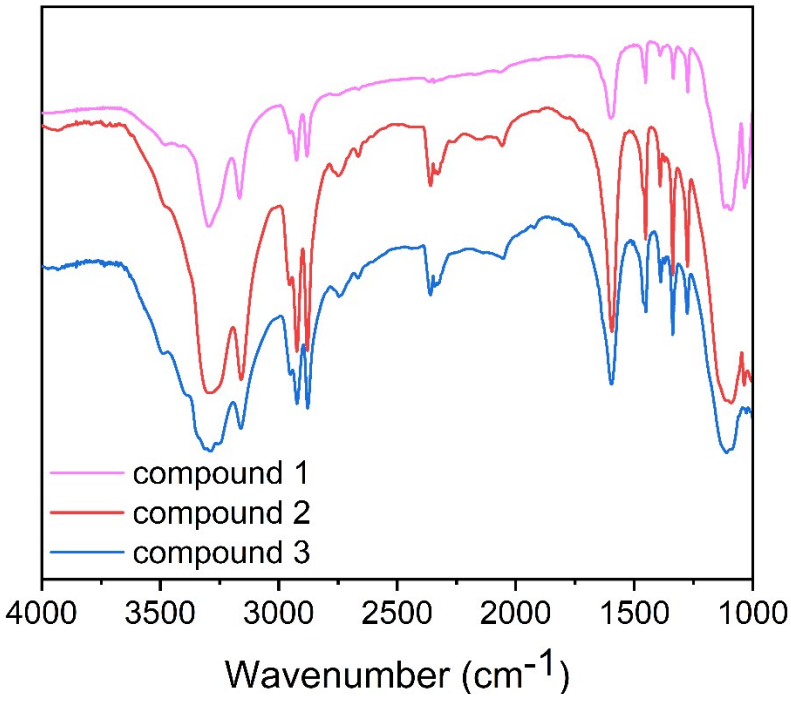

Figure S2. The IR spectra of **1**, **2**, **3** at room temperature.

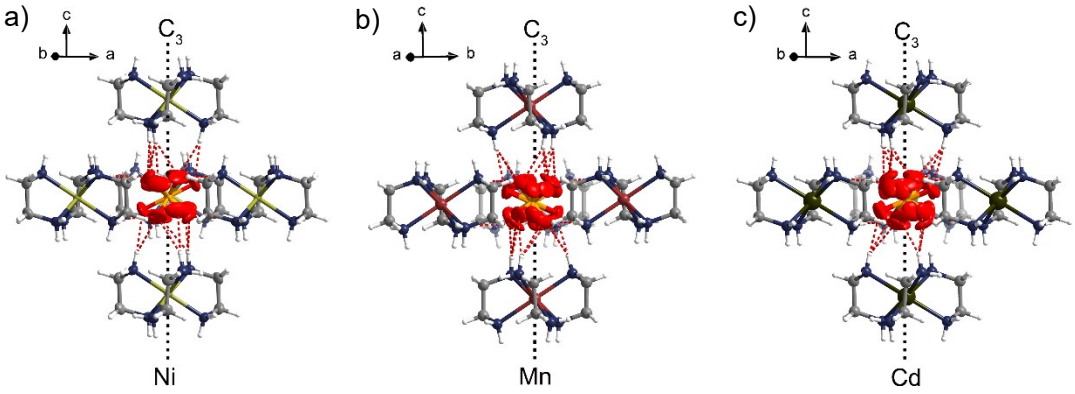

Figure S3. The structure of **1** (a), **2** (b), **3** (c) at the RTP, the SO_4^{2-} is located in a cavity composed of cations. The red dashed lines are the N–H···O hydrogen bond, and the black dashed lines are the C_3 axis parallel to the *c*-axis. The thermal ellipsoids of sulfate anions are drawn at a 50% probability level.

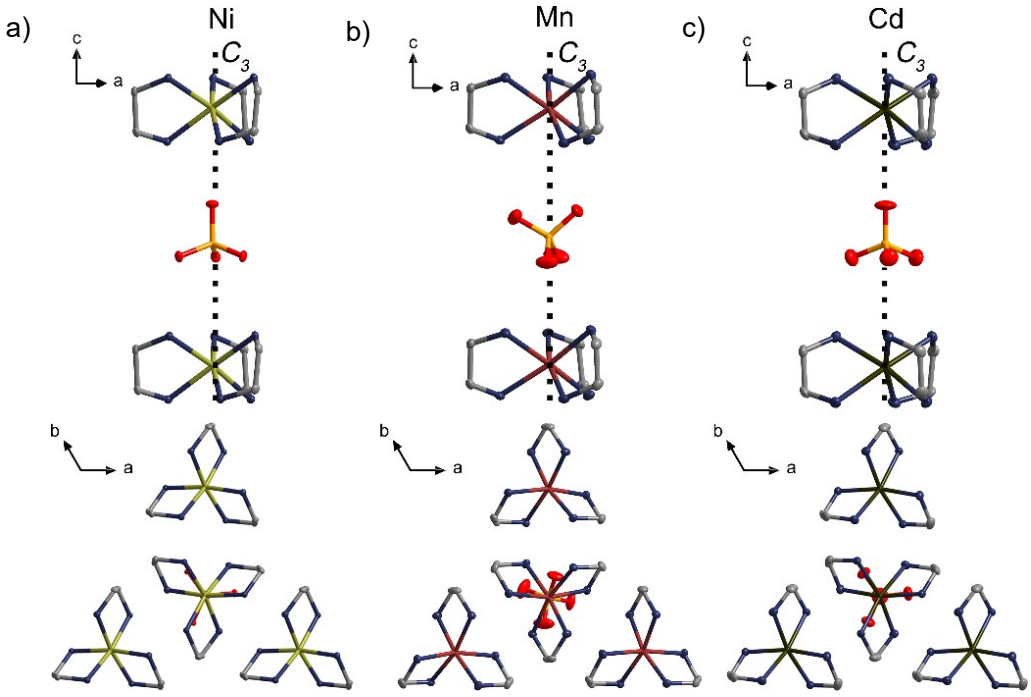

Figure S4. The structure difference of **1** (a), **2** (b) and **3** (c) at LTP. The thermal ellipsoids of sulfate anions are drawn at a 50% probability level. The hydrogen atoms are omitted for clarity.

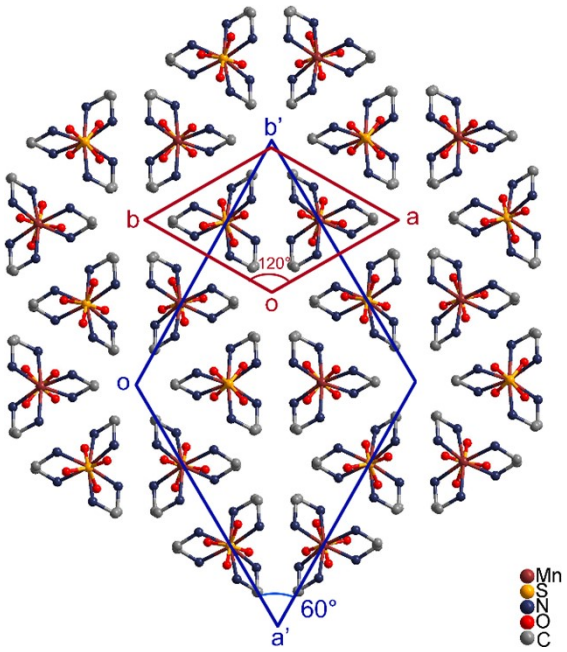

Figure S5. Unit cell change of **2** during phase transition. space group of crystal **2** changes to $P\bar{3}c1$ with a transformation in the lattice of

$$\begin{pmatrix} a \\ b \\ c \end{pmatrix}_{LTP} = \begin{pmatrix} 1.5 & \frac{\sqrt{3}}{2} & 0 \\ -\frac{\sqrt{3}}{2} & 1.5 & 0 \\ 0 & 0 & 1 \end{pmatrix} \times \begin{pmatrix} a \\ b \\ c \end{pmatrix}_{HTP}$$

The red box is the unit cell in the RTP, and the blue box is the unit cell in the LTP.

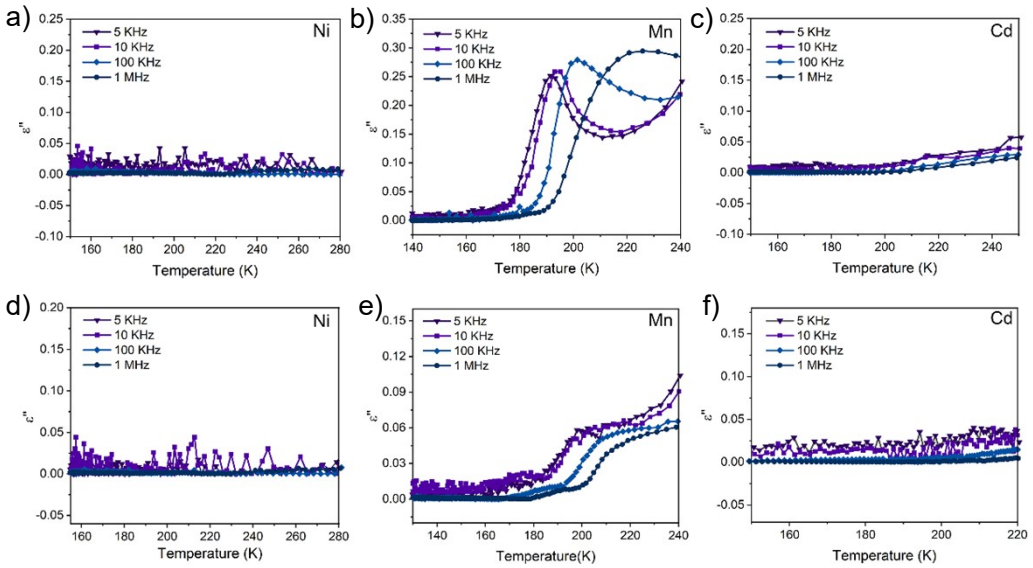

Figure S6. The dielectric loss in **1, 2**, and **3.** The dielectric loss measured along the *c* axis of **1** (a), **2** (b), and **3** (c). The dielectric loss measured along a direction perpendicular to the *c* axis of the single crystals of **1** (d), **2** (e), and **3** (f).

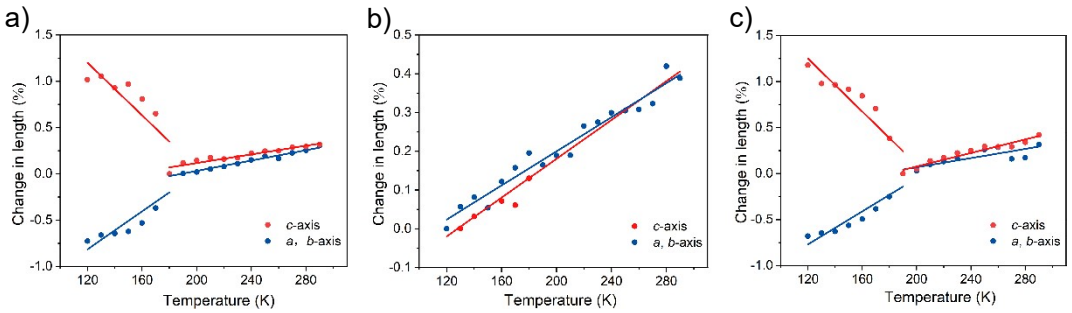

Figure S7. Anisotropic variation of thermal expansion of **1** (a), **2** (b), **3** (c) along the principal axis (*a*, *b*, *c*) obtained from *PASCal* in a certain temperature range[1]. All the cell lengths of these compounds gradually decrease upon cooling from room temperature to the phase transition temperature. The thermal expansion coefficients of the *a*, *b*, and *c* axes in **1** are $\alpha_{a,\ b} = 27.97 \times 10^{-6}$ K^{-1} and $\alpha_c = 23.46 \times 10^{-6}$ K^{-1}. The thermal expansion coefficients of each axis in **2** are $\alpha_{a,\ b} = 22.58 \times 10^{-6}$ K^{-1}, $\alpha_c = 25.37 \times 10^{-6}$ K^{-1}. The thermal expansion coefficients in **3** are $\alpha_{a,\ b} = 37.35 \times 10^{-6}$ K^{-1}, $\alpha_c = 24.90 \times 10^{-6}$ K^{-1}. **1** and **3** exhibit anisotropy in thermal expansion after the temperature is below the phase transition. The thermal expansion coefficients of **1** are $\alpha_{a',\ b'} = 103.44 \times 10^{-6}$ K^{-1} and $\alpha_{c'} = -140.54 \times 10^{-6}$ K^{-1}. The thermal expansion coefficients in **3** are $\alpha_{a',\ b'} = 90.40 \times 10^{-6}$ K^{-1} and $\alpha_{c'} = -142.13 \times 10^{-6}$ K^{-1}. The thermal expansion coefficient of **2** is almost unchanged, and it is an isotropic positive thermal expansion.

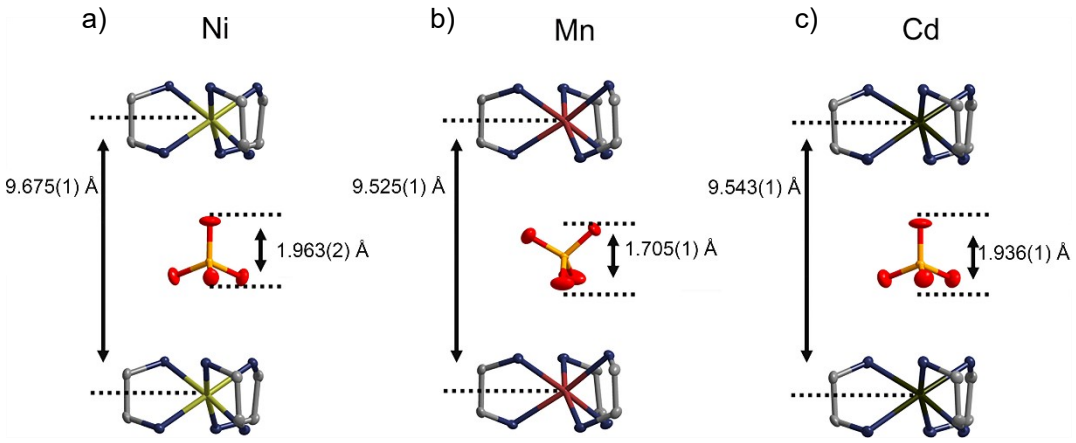

Figure S8. Lengths of SO_4^{2-} along the *c*-axis in **1** (a), **2** (b), **3** (c) in the LTP. The thermal ellipsoids of sulfate anions are drawn at a 50% probability level. The hydrogen atoms are omitted for clarity.

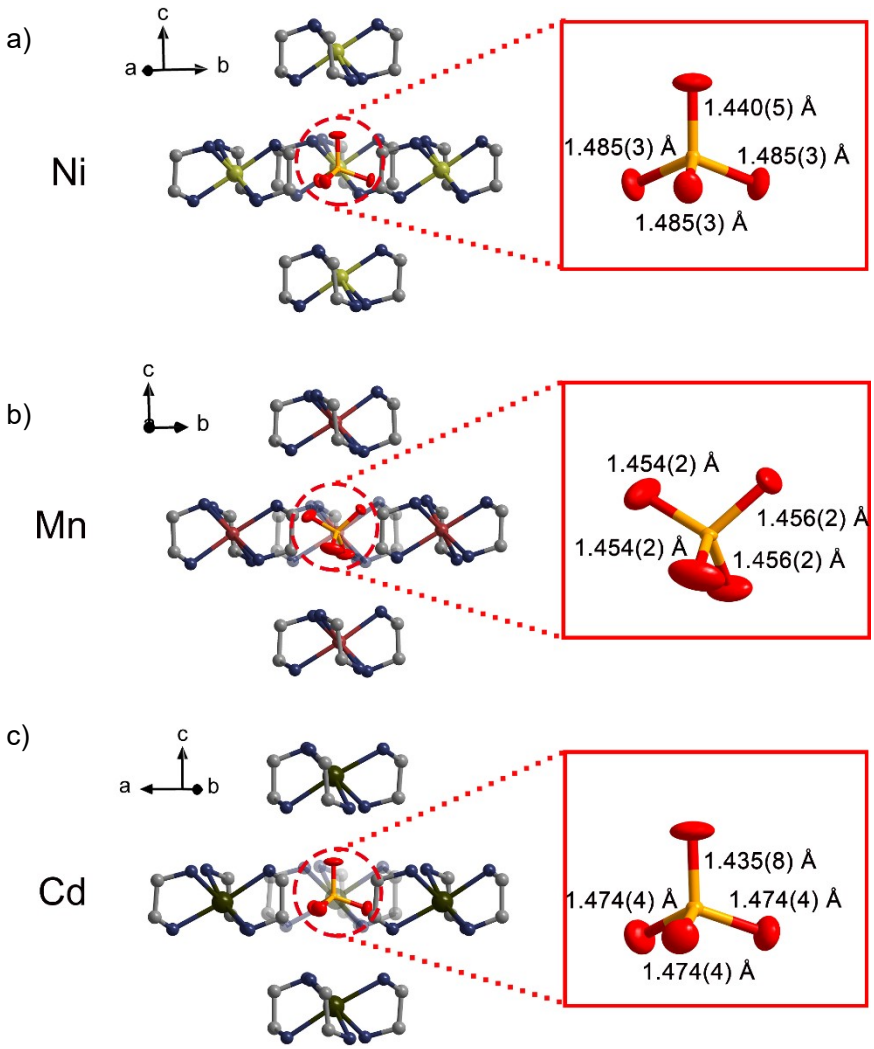

Figure S9. The structure of SO_4^{2-} in **1** (a), **2** (b), **3** (c) at the LTP. The bond lengths in the figure are the S–O bond length. The thermal ellipsoids of sulfate anions are drawn at a 50% probability level. The hydrogen atoms are omitted for clarity.

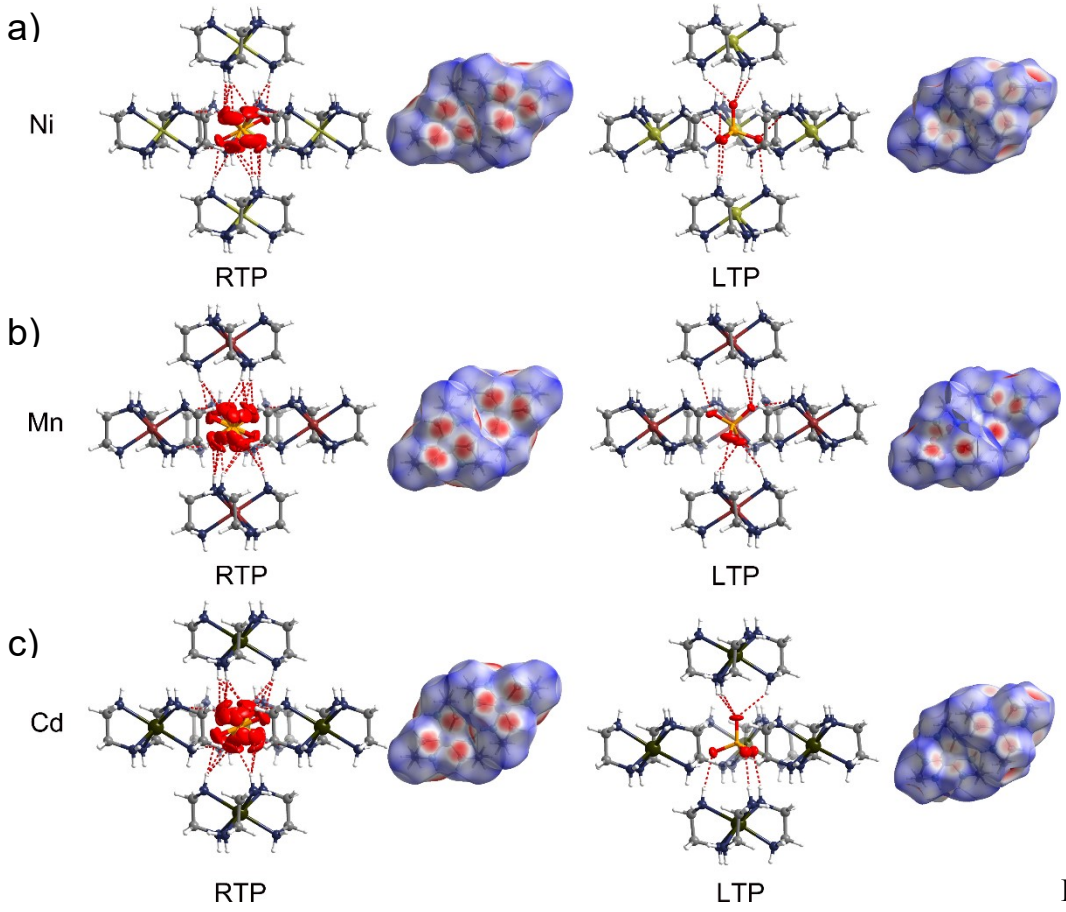

Fi gure S10. The hydrogen bonding environment of **1** (a), **2** (b), and **3** (c) in the RTP and the LTP. The Hirshfeld surface analyses[2] reveal the N–H···O hydrogen bond between the $[M^{II}(en)_3]^{2+}$ and the SO_4^{2-}.The red area in the figure indicates that the molecular contact is shorter than the van der Waals distance. In the RTP, the SO_4^{2-} in the three compounds are in dynamic disorder, and the range of hydrogen bonds in the direction parallel to the *c*-axis is mainly evenly distributed around the three N atoms.

In the LTP, the SO_4^{2-} in compounds **1** and **3** are in an upright state. It can be seen that the hydrogen bonds are close to the cation center, and the hydrogen bonds are weakened due to the increase of the distance between the adjacent cations. The SO_4^{2-} in compound **2** is in an tilt state, and the range of hydrogen bonds is still evenly distributed around the N atom.

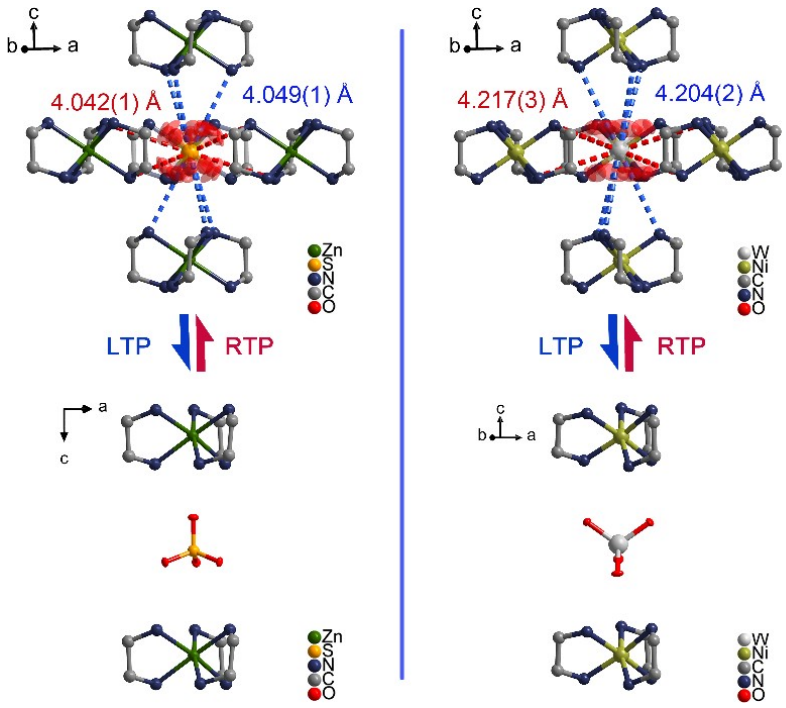

Figure S11. S···N or W···N distances in $[Zn^{II}(en)_3]$ SO_4 and $[Ni^{II}(en)_3]WO_4$. The thermal ellipsoids of Oxygen atom are drawn at a 50% probability level. The hydrogen atoms are omitted for clarity.

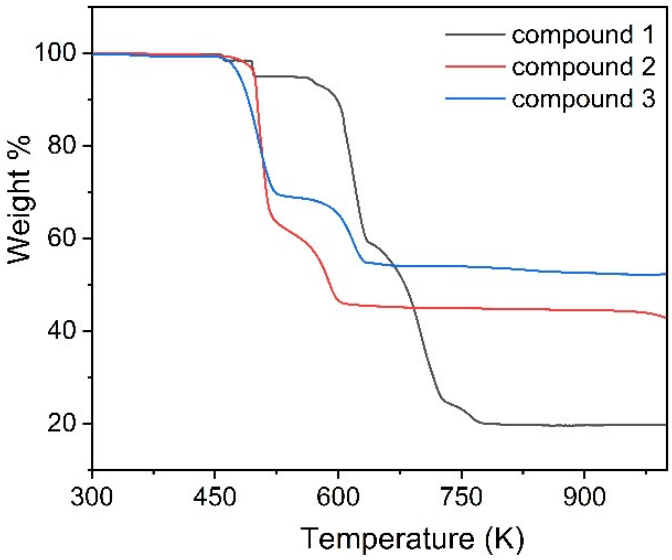

Figure S12. TG analysis of **1**, **2**, **3**.

Table S1. The crystallographic data for **1**–RTP, and **1**–LTP.

T / K	293 K (RTP)	140 K (LTP)
Empirical formula	$C_6H_{24}N_6O_4S_1Ni_1$	
Crystal system	trigonal	trigonal
Space group	$P\bar{3}1c$	$P\bar{3}$
a/Å	8.9389(5)	8.8526(4)
b/Å	8.9389(5)	8.8526(4)
c/Å	9.6152(5)	9.6749(4)
α/°	90	90
β/°	90	90
γ/°	120	120
Volume/Å^3	665.36(8)	656.63(7)
Dcalc.mg/m^3	1.669	1.695
μ/mm^{-1}	1.630	1.655
F_{000}	355.0	356.0
Reflections collected	3110	3355
Independent reflections	573	1095
R(int)	0.0286	0.0399
Data/restraints/parameters	573/0/42	1095/9/56
Goodness-of-fit on F^2	1.165	1.124
R_1[a] [I>=2σ (I)]	0.0299	0.0376
ωR_2[b] ([all data]	0.0764	0.0992

[a] $R1 = \sum||F_o| - |F_c||/\sum|F_o|$. [b] $wR_2 = \{\sum[w(F_o^2 - F_c^2)^2] / \sum[w(F_o^2)^2]\}^{1/2}$

Table S2. The crystallographic data for **2**–RTP and **2**–LTP.

T / K	293 K (RTP)	150 K (LTP)
Empirical formula	$C_6H_{24}N_6O_4S_1Mn_1$	
Crystal system	trigonal	trigonal
Space group	$P\bar{3}1c$	$P\bar{3}c1$
a/Å	9.0947(4)	15.6935(5)
b/Å	9.0947(4)	15.6935(5)
c/Å	9.5725(5)	9.5255(4)
α/°	90	90
β/°	90	90
γ/°	120	120
Volume/Å^3	685.70(7)	2031.69(16)
Dcalc.mg/m^3	1.605	1.625
μ/mm-1	1.133	1.147
F_{000}	350.0	1050.0
Reflections collected	3906	10980
Independent reflections	608	1809
R(int)	0.0320	0.0281
Data/restraints/parameters	608/0/41	1809/30/83
Goodness-of-fit on F^2	1.115	1.108
R_1[a] [I>=2σ (I)]	0.0290	0.0544
ωR_2[b] ([all data]	0.0788	0.1669

[a] $R1 = \sum||F_o| - |F_c||/\sum|F_o|$. [b] $wR_2 = \{\sum[w(F_o^2 - F_c^2)^2] / \sum[w(F_o^2)^2]\}^{1/2}$

Table S3. The crystallographic data for **3**–RTP and **3**–LTP.

T / K	293 K (RTP)	140 K (LTP)
Empirical formula	$C_6H_{24}N_6O_4S_1Cd_1$	
Crystal system	trigonal	trigonal
Space group	$P\bar{3}1c$	$P\bar{3}$
a/Å	9.1957(3)	9.1148(4)
b/Å	9.1957(3)	9.1148(4)
c/Å	9.5096(4)	9.5425(5)
α/°	90	90
β/°	90	90
γ/°	120	120
Volume/Å^3	696.41(5)	686.57(7)
Dcalc.mg/m^3	1.854	1.881
μ/mm-1	1.736	1.761
F_{000}	396.0	396.0
Reflections collected	3093	3365
Independent reflections	617	1144
R(int)	0.0490	0.0542
Data/restraints/parameters	617/0/41	1144/0/56
Goodness-of-fit on F^2	1.067	1.151
R_1[a] [I>=2σ (I)]	0.0294	0.0474
ωR_2[b] ([all data]	0.0756	0.1156

[a] $R1 = \sum||F_o| - |F_c||/\sum|F_o|$. [b] $wR_2 = \{\sum[w(F_o^2 - F_c^2)^2] / \sum[w(F_o^2)^2]\}^{1/2}$

Table S4. Bond lengths [Å] for **1** at 293 K and 140 K.

Temperature (K)	Bond lengths [Å]			
293 K	Ni1-N1	2.128(1)	N1-C1	1.475(3)
	C1-C1[5]	1.510(5)	O1-S1	1.453(7)
	O2-S1	1.424(6)		
140 K	Ni1-N1	2.130(3)	N1-C1	1.476(4)
	Ni1-N2	2.128(3)	O1-S1	1.485(3)
	C2-C1	1.518(5)	O2-S1	1.440(5)
	N2-C2	1.481(5)		

Symmetry codes: (5) +X, 1+X-Y, 3/2-Z.

Table S5. Bond lengths [Å] for **2** at 293 K and 150 K.

Temperature (K)	Bond lengths [Å]			
293 K	Mn1-N1	2.268(1)	N1-C1	1.467(2)
	O1-S1	1.445(5)	C1-C1[4]	1.515(3)
	O2-S1	1.419(6)		
150 K	Mn1-N3	2.260(2)	N3-C3	1.475(3)
	Mn1-N1	2.271(2)	N1-C1	1.476(3)
	Mn1-N2	2.278(2)	N2-C2	1.476(3)
	O1-S1	1.454(2)	C2-C1	1.516(4)
	S1-O2	1.456(2)	C3-C3[1]	1.520(5)

Symmetry codes: (4) 1+Y-X, +Y, 1/2-Z. (1) -X, -X+Y, 1/2-Z.

Table S6. Bond lengths [Å] for **3** at 293 K and 140 K.

Temperature (K)	Bond lengths [Å]			
293 K	Cd1-N1	2.362(2)	O2-S1	1.410(10)
	C1-C1[5]	1.501(5)	N1-C1	1.465(4)
	O1-S1	1.445(9)		
140 K	Cd1-N1	2.352(4)	N2-C2	1.467(6)
	Cd1-N2	2.372(4)	N1-C1	1.469(6)
	O1-S1	1.435(8)	C2-C1	1.524(7)
	O2-S1	1.474(4)		

Symmetry codes: (5) 1+Y-X, +Y, 3/2-Z.

References

1. M. J. Cliffe and A. L. Goodwin, *J. Appl. Crystallogr.*, 2012, **45**, 1321-1329.
2. J. J. Mckinnon, M. A. Spackman and A. S. Mitchell, *Acta Cryst B.*, 2004, **60**, 627-668.